

# Lawrence Berkeley National Laboratory

## LBL Publications

### Title

Thermal Pressure in the Thermal Equation of State for Solid and a Proposed Substitute

### Permalink

<https://escholarship.org/uc/item/83d5m9s0>

### Journal

International Journal of Thermophysics, 43(11)

### ISSN

0195-928X

### Authors

Yan, Jinyuan

Yang, Shizhong

### Publication Date

2022-11-01

### DOI

10.1007/s10765-022-03089-8

### Copyright Information

This work is made available under the terms of a Creative Commons Attribution License, available at

<https://creativecommons.org/licenses/by/4.0/>

Peer reviewed



# Thermal Pressure in the Thermal Equation of State for Solid and a Proposed Substitute

Jinyuan Yan<sup>1</sup> · Shizhong Yang<sup>2</sup>

Received: 11 July 2022 / Accepted: 20 August 2022 / Published online: 14 September 2022  
© The Author(s) 2022, corrected publication 2022

## Abstract

The thermal equation of state (TEOS) for solids is a mathematic model among pressure, temperature and density, and is essential for geophysical, geochemical, and other high pressure–temperature (high P–T) researches. However, in the last few decades, there has been a growing concern about the accuracy of the pressure scales of the calibrants, and efforts have been made to improve it by either introducing a reference standard or building new thermal pressure models. The existing thermal equation of state,  $P(V, T) = P(V, T_0) + P_{th}(V, T)$ , consists of an isothermal compression and an isochoric heating, while the thermal pressure is the pressure change in the isochoric heating. In this paper, we demonstrate that, for solids in a soft pressure medium in a diamond anvil cell, the thermal pressure can neither be determined from a single heating process, nor from the thermal pressure of its calibrant. To avoid the thermal pressure, we propose to replace the thermal pressure with a well-known thermal expansion model, and integrate it with the isothermal compression model to yields a Birch–Murnaghan-expansion TEOS model, called VPT TEOS. The predicted pressure of MgO and Au at ambient pressure from Birch–Murnaghan-expansion VPT TEOS model matches the experimental pressure of zero (0) GPa very well, while the pressure prediction from the approximated Anderson PVT TEOS exhibit a big deviation and a wrong trend.

**Keywords** Condensed matter · Isobaric · Isochoric · Isothermal · PVT TEOS · Thermal equation of state (TEOS) · VPT TEOS

---

✉ Jinyuan Yan  
jyan@lbl.gov

<sup>1</sup> Material Science Division, Lawrence Berkeley National Lab, Berkeley, CA, USA

<sup>2</sup> Department of Computer Science, Southern University and A&M College, Baton Rouge, LA, USA

## 1 Introduction

The thermal equation of state (TEOS) is a mathematical expression among the thermophysical properties of solids, including temperature, pressure, and density. It is essential for interpreting geophysical and material science observations. However, there have been extensive controversies in the accuracy of the pressure scales, and large discrepancies in pressure determination using different pressure standards or different thermal equations of state for the same standard have been reported [1–5]. The uncertainty in the pressure scale has led to a large controversy on the origins of seismic velocity discontinuities [3]. The existing TEOS  $P(V, T) = P(V, T_0) + P_{th}(V, T)$ , called PVT TEOS, consists of two constituents, one isothermal compression pressure at room temperature, and one isochoric heating at high pressure. The isothermal compression term has been well-established and well accepted by the high pressure–temperature (high P–T) community, while efforts have been made to improve the thermal pressure term by either introducing a reference standard [1], inter-calibration [4], or building new thermal pressure models [6–11].

The first and the most popular thermal pressure model is the Anderson model [12, 13],  $P_{th} = \int \alpha_p K_T dT$ , an integral of the product of thermal expansion coefficient  $\alpha_p$  and bulk modulus  $K_T$  over a temperature range. Since both  $\alpha_p$  and  $K_T$  are temperature and pressure dependent, and both are cross-linked, the mathematical integration of  $\alpha_p \cdot K_T$  is not straightforward. The most popular solution is to simplify it and reduce the product of  $\alpha_p \cdot K_T$  to  $\alpha_0 \cdot K_0$ . As  $\alpha_0 \cdot K_0$  is both pressure independent and temperature independent, the integration of  $\alpha_0 \cdot K_0$  at high P–T become possible, while this approximation brings in some error. To fix this deviation, the approximation induced pressure scale error will be investigated at ambient pressure up to 1400 K. In addition, there are a variety of other thermal pressure models, such as Maxwell relation [14], first-principles and molecular dynamics [6, 7, 15], Mie–Grüneisen–Debye [4, 8], finite elements [9, 10], and Holland and Powell [11]. To prove these models, experimentally determined thermal pressure are required.

In this report, the thermal pressure from experiment perspective is discussed and a thermal expansion model is proposed to replace the thermal pressure model. A Birch–Murnaghan-expansion VPT TEOS is proposed and its validation at ambient pressure is presented.

## 2 Thermal Pressure at High P–T Conditions in PVT TEOS

### 2.1 The Thermal Pressure is the Pressure Change in an Isochoric Heating

The textbook “Equations of State of Solids for Geophysics and Ceramic Science” [13] has become a guideline for the principles, theory, and practical application of thermal equations of state (TEOS) [16]. In this book, thermal pressure is

considered as the pressure required to keep the volume constant when the temperature is raised. In other words, the thermal pressure is the pressure change in an isochoric heating process [12, 13]. In 1968, Anderson [17] developed his thermal pressure equation from an isobaric heating and an isothermal compression. According to thermal expansion law, solids of positive thermal expansion coefficient expand when heated either under pressure or under ambient. Anderson equations [17] are rewritten as  $V = V(T, P)$ , as shown below

$$dV = \left(\frac{\partial V}{\partial P}\right)_T dP + \left(\frac{\partial V}{\partial T}\right)_P dT. \tag{1}$$

To get an isochoric heating, i.e.,  $dV = 0$

$$0 = \left(\frac{\partial V}{\partial P}\right)_T dP + \left(\frac{\partial V}{\partial T}\right)_P dT, \tag{2}$$

By introducing the definition of bulk modulus  $\left(\frac{\partial V}{\partial P}\right)_T = -\frac{V}{K_T}$  and the definition of thermal expansion coefficient  $\left(\frac{\partial V}{\partial T}\right)_P = V * \alpha_P$ , Eq. 2 is transformed to  $\left(\frac{\Delta P}{\Delta T}\right)_V = \alpha * K$ , then integrate over temperature and get

$$P_{th} = \int_{T_1}^{T_2} (\alpha * K) dt. \tag{3}$$

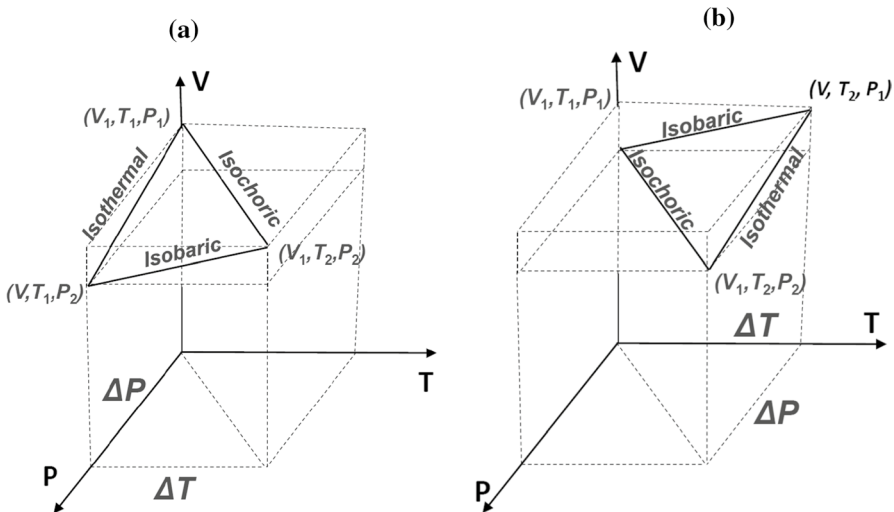


**Fig. 1** Schemes of isochoric processes. In (a), an isothermal compression and an isobaric heating make an isochoric process. In (b), an isobaric heating plus an isothermal compression generate an isochoric process. Both (a) and (b) demonstrate that an isochoric process is not a regular heating process, but a combination of heating and compression

According to Eq. 2, to get an isochoric process, volume change by the  $\left(\frac{\partial V}{\partial P}\right)_T dP$  in an isothermal compression process has to be canceled by  $\left(\frac{\partial V}{\partial T}\right)_P dT$  in a subsequent isobaric heating process. The isothermal compression process and isochoric process are illustrated in Fig. 1(a). To keep volume constant after heating, pressure needs to be adjusted accordingly, as illustrated in Fig. 1(b). In other words, an isochoric process can only be achieved by a dual process which consists of isobaric heating and an isothermal compression; any single isobaric/non-isobaric heating process cannot be practically reached at high pressure. By Eqs. 2 and 3, the thermal pressure is the pressure pushing the sample's volume back to the volume prior to heating. As a result, in any heating process which is approximated to be isochoric, its thermal pressure should be zero. For any sample whose thermal expansion coefficient is zero, its thermal pressure should be zero.

To experimentally measure thermal pressure, one has to construct an isochoric heating process first, then measure the pressure change in this isochoric process. An isochoric heating can be easily achieved for a gas or fluid, but not for a solid sample in a pressure medium such as a diamond anvil cell (DAC) or large volume press (LVP) [5, 18, 19]. As Eqs. 2 and 3, the thermal pressure is the integration of the product of  $\alpha_p \cdot K_T$  in an isochoric heating process. In the isochoric heating process, (1) temperature and pressure are changed accordingly, (2) both  $\alpha_p$  and  $K_T$  are temperature and pressure dependent, and are inter-cross-linked, so the integration on  $\alpha_p \cdot K_T$  is not straightforward.

In early low and moderate pressure–temperature experiments using DACs, thermal expansion of the DACs and sample chambers were negligible, so the heated sample was considered to be under isochoric conditions. The pressure changes during heating in these experiments were assumed to be thermal pressure [20–22]. However, an isochoric sample chamber is not an isochoric sample. It has been reported that regular resistive heating at high pressure is not isochoric [23–25], but partially isochoric [5], or intermediate between isochoric and isobaric [26]. Precisely speaking, for a DAC, the pressure change during a non-isochoric heating is not exactly the thermal pressure. The inaccurate thermal pressure assumptions from non-isochoric processes might be the main error source, causing the discrepancies among the common pressure standards.

Thermal pressure was suggested to measure the pressure change along the isochoric contour [23, 27, 28], but constructing an isochoric contour is a challenge.

## 2.2 Thermal Pressure of a Sample Cannot be Determined from a Calibrant

From  $P_{th} = \int \alpha_p K_T dT$ ,  $\alpha_{sample} \neq \alpha_{calibrant}$ , and  $K_{sample} \neq K_{calibrant}$ , we have:

$$\int \alpha_{sample} K_{sample} dT \neq \int \alpha_{calibrant} K_{calibrant} dT. \quad (4)$$

The Eq. 4 shows that the  $P_{th}$  of the sample does not equal the  $P_{th}$  of a pressure calibrant. Thermal pressure in Eq. 3 is a process variable over a temperature, not a state

variable. The above argument demonstrates that a calibrant's thermal pressure cannot be used as sample's the thermal pressure determination in the heating process, even at each state, the pressure of a calibrant equals to the pressure of a sample. As a conclusion, measuring the sample's thermal pressure from its pressure marker is not accurate.

### 2.3 Thermal Pressure, Grüneisen Parameter, and High $T$ Bulk Modulus Fitting

Thermal pressure is the pressure change in isochoric heating in a certain temperature range. Even the pressure at high  $P$ - $T$  can be determined by a calibrant, but the sample's thermal pressure doesn't equal its calibrant's thermal pressure. For the solid in a soft pressure medium, an isochoric heating can be accomplished by a compression after a heating, and a single heating process at high  $P$ - $T$  is not an isochoric, and thermal pressure cannot be determined directly from a single heating process. This might be the reason why pressure accuracy at high  $P$ - $T$  has not been consistent widely.

In addition to the Anderson thermal pressure model, another most popular model to calculate the thermal pressure is called Mie-Grüneisen-Debye, where The Grüneisen parameter,  $\gamma$ , named after Eduard Grüneisen, describes the effect that changing the volume of a crystal lattice has on its vibrational properties. Even though there are various ways to calculate the Grüneisen parameter, accurate thermal pressure is required to validate the Mie-Grüneisen-Debye model. Similarly, accurate thermal pressure is required to fit temperature dependent bulk modulus as well.

## 3 Thermal Expansion Model at High $P$ - $T$ Conditions

In Sect. 2, we demonstrate that a single heating for DAC is not isochoric process, and the pressure determined from a non-isochoric heating process is not exact its thermal pressure. On the contrary, isobaric heating for diamond anvil cell at high pressure have been reported [29–38], either with aid of membrane for a DAC or by adjusting the load for an LVP. Pressure dependent thermal expansion is the thermal expansion process in an isobaric heating process. In reference [39], Yan and Yang proposed a revertible heating/cooling process to measure pressure dependent thermal expansion coefficient by a diamond anvil cell experimentally, when a diamond anvil cell is equipped with a membrane. In a revertible heating/cooling technique, an isobaric process was justified as the heating data and cooling data are revertible, and no pressure determination at high  $P$ - $T$  during heating is required, and thus it eliminates the pressure measuring issue at high  $P$ - $T$  conditions.

In next section, thermal expansion will be combined with isothermal compression, yielding Birch-Murnaghan-thermal expansion model.

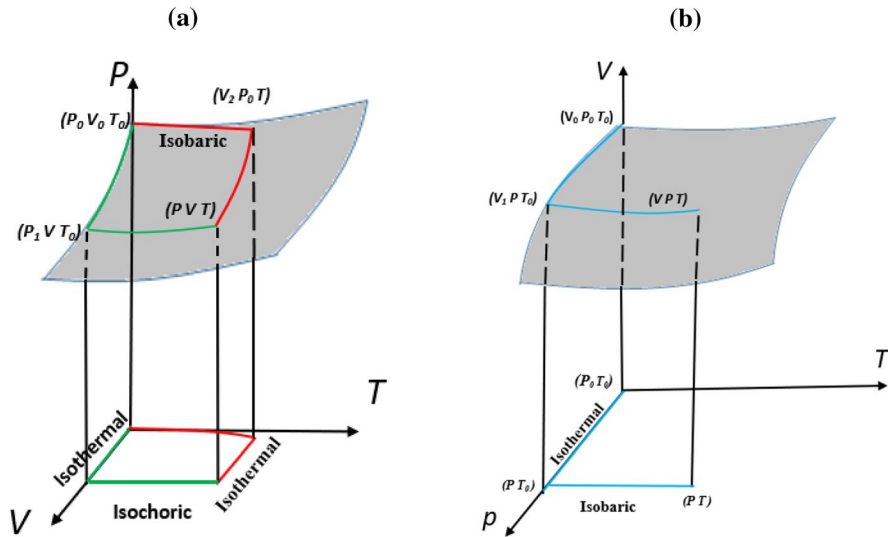


**Fig. 2** Schematic to build the mathematical relation between  $P$ ,  $V$ , and  $T$ . In (a), the pressure is a function of volume and temperature. The green pathway represents the typical PVT TEOS. In (b), the volume is a function of pressure and temperature. The red pathway indicates a model consisting of isobaric heating at ambient pressure and isothermal compression under high temperature. The blue pathway of VPT TEOS consists of an isothermal compression at room temperature and an isobaric heating at high pressure (Color figure online)

#### 4 VPT TEOS and Birch–Murnaghan-Expansion VPT TEOS

In the existing TEOS, pressure ( $P$ ) is expressed as a function of volume ( $V$ ) and temperature ( $T$ ), and this might be the reason why this TEOS is called PVT TEOS. The pathway of developing a PVT TEOS is illustrated in Fig. 2a along the green pathway. In addition to PVT TEOS, another thermal equation of state along the red pathway in Fig. 2(a) was reported [40–42]. Along the red pathway, it consists an isobaric heating at ambient pressure and an isothermal compression at high temperature. To differentiate the red pathway with the green pathway of PVT TEOS, we call the red pathway model PTV TEOS. For the PTV TEOS, there is no thermal pressure term, but measuring reliable pressure,  $K_T$ , and  $K'_T$  at high P–T is a big challenge.

In addition to green pathway PVT TEOS, and red pathway PTV TEOS, we propose a blue pathway in Fig. 2(b). In this model, the volume ( $V$ ) is expressed as a function of pressure ( $P$ ) in the isothermal compression and a function of temperature ( $T$ ) in the isobaric heating, so, we name the blue pathway model VPT TEOS. The beginning state ( $V_0, P_0, T_0$ ), the intermediate state ( $V_1, P, T_0$ ), and the final state ( $V, P, T$ ) are illustrated in Fig. 2(b). Along the blue pathway, temperature remains constant in the isothermal compression process from the initial state ( $V_0, P_0, T_0$ ) to intermediate state ( $V_1, P, T_0$ ), while the pressure remains constant in the process from the intermediate state to the final state. The advantage of the blue pathway over

the red pathway is that no pressure determination at high temperature is required, and both volume and temperature are easily measured.

Along the blue pathway of the VPT TEOS, the isothermal compression from the beginning state  $(V_0, P_0, T_0)$  to the intermediate state  $(V_1, P, T_0)$  can be expressed by various models, such as Murnaghan [43], modified Tait [44], natural strain [45], Vinet [46], Birch–Murnaghan [47], and others. The general form of all of these isothermal compression models is the pressure ( $P$ ) as a function of the volume ( $V$ ),

$$P = f^{-1}(T_0, V_1, V_0, K_0, K'_0). \quad (5)$$

Here  $P$  is the pressure value at the intermediate state  $(V_1, P, T_0)$ , and  $V_1$  is the volume at the intermediate state  $(V_1, P, T_0)$ , illustrated in Fig. 2(b). Subscript 0 refers to the initial state, and subscript 1 refers to the intermediate state. The inverse function of Eq. 5 is expressed as

$$V_1 = f(T_0, P, V_0, K_0, K'_0). \quad (6)$$

In the isobaric heating process from the intermediate state  $(V_1, P, T_0)$  to the final state  $(V, P, T)$ , the volume at  $(V, P, T)$  can be solved using the isobaric thermal expansion process,

$$V = V_1 \times \exp\left(\int_{T_0}^T \alpha_p \cdot dx\right). \quad (7)$$

In Eq. 7,  $x$  is the integral variable from  $T_0$  to  $T$ .  $\alpha_p$  is the pressure dependent thermal expansion coefficient, and also it is a function of temperature. Substituting volume  $V_1$  in Eq. 7 with  $V_1$  in Eq. 6 yields

$$V = f(T_0, P, V_0, K_0, K'_0) \cdot \exp\left(\int_{T_0}^T \alpha_p \cdot dx\right). \quad (8)$$

In Eq. 8, the volume ( $V$ ) is a function of pressure ( $P$ ) and temperature ( $T$ ), and this is the reason why this TEOS is called VPT TEOS, and has no thermal pressure term in it.

The coefficients in these three different TEOSs are different: (1) the coefficients for green pathway PVT TEOS are  $\alpha_p$ ,  $K_T$ , and  $K_0$ ; (2) the coefficients for red pathway PTV TEOS are  $\alpha_0$ ,  $K_T$  and  $K_T$ ; and (3) the coefficients for blue pathway VPT TEOS are  $\alpha_p$ ,  $K_0$ , and  $K_0$ .

To simplify Eq. 8, divide  $\exp\left(\int_{T_0}^T \alpha_p \cdot dx\right)$  into both sides, and get

$$V \cdot \exp\left(-\int_{T_0}^T \alpha_p \cdot dx\right) = f(T_0, P, V_0, K_0, K'_0). \quad (9)$$

Set  $V \cdot \exp\left(-\int_{T_0}^T \alpha_p \cdot dx\right)$  on the left side as  $V_M$ , where M is called modified volume,



$$V_M = V \cdot \exp\left(-\int_{T_0}^T \alpha_p \cdot dx\right) \tag{10}$$

and Eq. 9 becomes

$$V_M = f(T_0, P, V_0, K_0, K'_0). \tag{11}$$

The Eq. 11 gives the general form of VPT TEOS for volume at high pressure high temperature. It describes the mathematical relationship between volume, pressure, and temperature for solids in a pressure medium. It has the same ‘‘appearance’’ as the isothermal compression in Eq. 6 except the modified volume on the left side. The inverse function of Eq. 11 is

$$P = f^{-1}(T_0, V_M, V_0, K_0, K'_0). \tag{12}$$

The Eq. 12 is the general form of the VPT TEOS for pressure at a given temperature and volume. It has the same appearance as the isothermal compression in Eq. 5 except that its volume is replaced by the modified volume.

Taking the 3<sup>rd</sup> order Birch–Murnaghan equation as an example,  $P$  can be solved for a given volume ( $V$ ) and temperature ( $T$ ) by:

$$P_{V,T} = \frac{3K_0}{2} \left[ \left( \left( \frac{V_0}{V_M} \right)^{\frac{2}{3}} \right) - \left( \frac{V_0}{V_M} \right)^{\frac{5}{3}} \right] \left\{ 1 + \frac{3}{4}(K'_0 - 4) \left[ \left( \left( \frac{V_0}{V_M} \right)^{\frac{2}{3}} \right) - 1 \right] \right\}. \tag{13}$$

The Eq. 13 describes a specific form of mathematical relationship among pressure, volume, and temperature based on the 3rd order Birch–Murnaghan model, called Birch–Murnaghan-expansion VPT TEOS model.

One issue is that, to calculate the pressure from Eq. 13 for any ( $V, T$ ) data, the unknown pressure,  $P_{V,T}$ , is on the left side of Eq. 13, and the unknown pressure associated thermal expansion coefficient on the right side as well, so there is no pressure analytical solution. However, for any known monotonic alpha ( $P$ ), the pressure monotonically decreases with volume, and there is only one pressure numeric analysis solution corresponding to a specific volume value at specific temperature, so the pressure can be solved by any small computer code. For example, (1) choose a reasonable ( $P_1, P_2, \dots, P_n$ ) range, it yield to a ( $\alpha_1, \alpha_2, \dots, \alpha_n$ ) array, (2). integrate the  $\alpha$  array into Eq. 13 with given ( $V, T$ ), and solve a calculated pressure array ( $P^*1, P^*2, \dots, P^*n$ ), (3) find the numerical solution which fall into the preset threshold. Similarly, there is no analytical solution but a numerical solution for the general volume expression of Eq. 11 and general pressure expression of Eq. 12 of VPT TEOS.

In summary, the VPT TEOS consists of one isothermal compression at room temperature and one isobaric thermal expansion at high pressure. There is no thermal pressure term in it. The general form of VPT TEOS for pressure looks like the same as the isothermal compression expression of Eq. 5 except the modified volume in it.

## 5 Validation of Birch–Murnaghan-Expansion VPT TEOS and Comparison with Birch–Murnaghan-Approximated Anderson PVT TEOS at Ambient Pressure

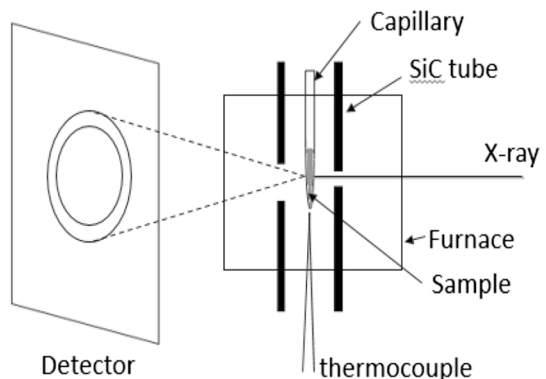
### 5.1 Experiments

As discussed in Sect. 2.1, in an isochoric heating process over a certain temperature range, (1) both  $\alpha_p$  and  $K_T$  are temperature dependent and pressure dependent, and both are cross-linked, (2) temperature and pressure are changed accordingly to achieve an isochoric heating, as a result, the integration on of  $\alpha_p \cdot K_T$  is not straightforward. To simplify, the product of  $\alpha_p \cdot K_T$  is reduced to  $\alpha_0 \cdot K_0$  [13, 41, 48, 49]. In this section, the reduced  $\alpha_0 \cdot K_0$  refers to the approximated thermal pressure. For the VPT TEOS, since  $\alpha_0$  at ambient pressure for most pressure calibrants are available, and limited  $\alpha_p$  at high pressure, the verification of the Birch–Murnaghan-expansion VPT TEOS model will be constrained to ambient pressure in this study. This is the reason why we specifically add “at ambient pressure” to the title. In this section, the comparison of both Birch–Murnaghan-expansion VPT TEOS and Birch–Murnaghan-Approximated Anderson PVT TEOS results at ambient pressure will be introduced.

For the high P–T experiments, volume and temperature are measured directly and accurately, while pressure at high P–T is calculated by a TEOS. At the moment, the pressures calculated from PVT TEOS at high P–T are not consistent [1–5], but the pressure of ambient pressure (0 GPa) itself is accurate and well accepted. To validate the VPT TEOS model at ambient pressure, we collect a reliable MgO ( $V$ ,  $P$ ,  $T$ ) dataset at ambient pressure, predict pressure using Birch–Murnaghan-expansion VPT TEOS and Birch–Murnaghan-Approximated Anderson PVT TEOS, and compare the predicted pressure values with the ambient pressure of zero (0) GPa.

An accurate volume of MgO was collected by synchrotron X-ray diffraction (XRD), in beamline 12.2.2 at advanced light source (ALS), Lawrence Berkeley National Laboratory [50]. The sample was loaded in a capillary, and its pressure in the open capillary was 1 bar (0.0001 GPa). The sample temperature was measured by a thermocouple. Figure 3 shows the schematic experimental setup, and more

**Fig. 3** The schematic experimental setup



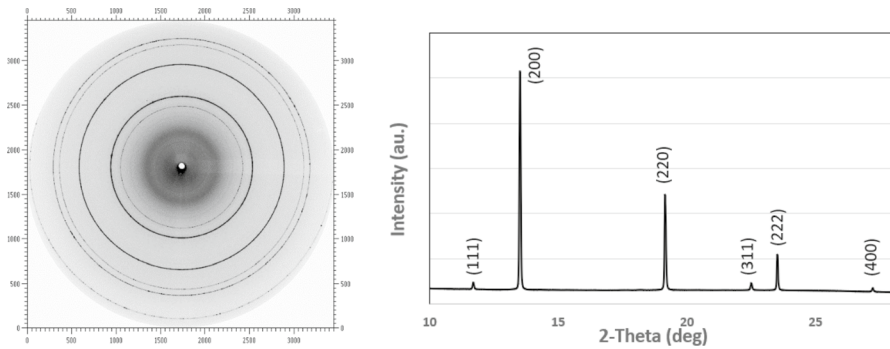


**Fig. 4** Left: The 2D X-ray diffraction pattern at 473 K; Right: the integration of the left pattern

**Table 1** Experimental temperature, volume, and pressure, along with model prediction pressure from Birch–Murnaghan-expansion VPT TEOS, and Birch–Murnaghan-Approximated Anderson PVT TEOS

Exp. temperature (K)	Exp. volume ( $\text{\AA}^3$ )	Exp. pressure (GPa)	VPT TEOS predicted P (GPa) <sup>c</sup>	PVT TEOS predicted P (GPa) <sup>d</sup>
298	$74.6 \pm 0.023$	0.0	$0.00 \pm 0.01$	$0.00 \pm 0.1$
473	$75.0 \pm 0.011$	0.0	$0.13 \pm 0.05$	$0.14 \pm 0.05$
573	$75.3 \pm 0.008$	0.0	$0.15 \pm 0.03$	$0.19 \pm 0.03$
673	$75.7 \pm 0.009$	0.0	$0.11 \pm 0.04$	$0.18 \pm 0.04$
773	$76.0 \pm 0.008$	0.0	$0.06 \pm 0.03$	$0.17 \pm 0.03$
873	$76.3 \pm 0.013$	0.0	$0.02 \pm 0.05$	$0.20 \pm 0.05$
973	$76.6 \pm 0.014$	0.0	$0.08 \pm 0.06$	$0.31 \pm 0.05$
1073	$77.0 \pm 0.026$	0.0	$0.05 \pm 0.11$	$0.36 \pm 0.1$
1173	$77.2 \pm 0.03$	0.0	$0.11 \pm 0.12$	$0.50 \pm 0.11$
1023 <sup>a</sup>	$76.8 \pm 0.015$	0.0	$0.14 \pm 0.06$	$0.40 \pm 0.06$
823 <sup>a</sup>	$76.1 \pm 0.017$	0.0	$0.11 \pm 0.07$	$0.25 \pm 0.07$
623 <sup>a</sup>	$75.5 \pm 0.021$	0.0	$0.14 \pm 0.09$	$0.19 \pm 0.08$
423 <sup>a</sup>	$74.9 \pm 0.023$	0.0	$0.12 \pm 0.10$	$0.13 \pm 0.1$
323 <sup>a</sup>	$74.6 \pm 0.024$	0.0	$0.02 \pm 0.1$	$0.02 \pm 0.1$
1223 <sup>b</sup>	77.4	0.0	0.07	0.51
1323 <sup>b</sup>	77.7	0.0	0.07	0.61
1423 <sup>b</sup>	78.1	0.0	0.07	0.72

<sup>a</sup>Indicated that the data were collected when cooling

<sup>b</sup>Indicated that the data were extrapolated

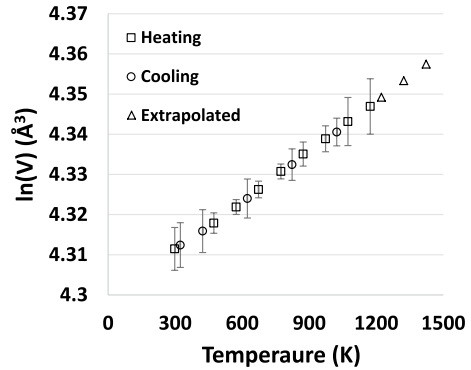
<sup>c</sup>Pressure predicted from  $P_{V,T} = \frac{3K_0}{2} \left[ \left( \left( \frac{V_0}{V_M} \right)^{\frac{2}{3}} \right) - \left( \frac{V_0}{V_M} \right)^{\frac{5}{3}} \right] \left\{ 1 + \frac{3}{4} (K'_0 - 4) \left[ \left( \left( \frac{V_0}{V_M} \right)^{\frac{2}{3}} \right) - 1 \right] \right\}$ , where

$$V_M = V \cdot \exp\left(-\int_{T_0}^T \alpha_p \cdot dx\right)$$

<sup>d</sup>Pressure predicted

$$\text{from } P_{V,T} = \frac{3K_0}{2} \left[ \left( \left( \frac{V_0}{V} \right)^{\frac{2}{3}} \right) - \left( \frac{V_0}{V} \right)^{\frac{5}{3}} \right] \left\{ 1 + \frac{3}{4} (K'_0 - 4) \left[ \left( \left( \frac{V_0}{V} \right)^{\frac{2}{3}} \right) - 1 \right] \right\} + \alpha_0 \cdot K_0 (T - T_0)$$

**Fig. 5** The volume vs. temperature of solid MgO in a capillary



detail of the setup is available in ref. [51]. During the heating/cooling process, a 100  $\mu\text{m}$  diameter open capillary was used, heated up to 1173 K, and then cooled down to room temperature. Angle-dispersive diffraction data were collected at an energy of 25 keV with a well-focused ( $10 \times 10 \mu\text{m}^2$  spot size) synchrotron X-ray beam. The XRD patterns were collected from a MAR345 image plate. Sample volumes were fitted by the method of Celref [52]. A 2-D XRD images at 473 K and its integrated XRD patterns show in Fig. 4. The experimental data of temperature, volume, and pressure are listed in Table 1 as “Exp. Temperature (K)”, “Exp. Volume ( $\text{\AA}^3$ )”, and “Exp. Pressure (GPa)”, respectively, and plotted in Fig. 5.

The unit cell volume at room temperature from this study is  $74.55 \text{\AA}^3$ , which is very close to the  $74.56 \text{\AA}^3$  ( $11.227 \text{cm}^3/\text{mole}$ ) [53]. Both heating data and cooling data are plotted in Fig. 5. To extend its temperature range, 3 extra data points are extrapolated, listed in Table 1 as double star (\*\*), and plotted in Fig. 5 as triangles. The zero order of thermal expansion coefficient of MgO from 297 to 1173 K was fitted as  $4.13 \pm 0.04 \times 10^{-5} \text{K}^{-1}$ , and it agrees with the experiment data in ref. [54].

## 5.2 Validation of Birch–Murnaghan–Expansion VPT TEOS

To validate the VPT TEOS model, we predict the pressure of MgO from the model and check if the predicted pressure matches the experimental value of zero (0) GPa. The inputs for Eq. 13 are the experimental MgO volume and temperature in Table 1, the bulk modulus  $K_0$  of 160.2 GPa, pressure derivative bulk modulus  $K'_0$  of 3.99,  $V_0$  of  $74.55 \text{\AA}^3$  fitted from our data, and the thermal expansion coefficient at ambient pressure  $\alpha_0$  of  $4.13 \pm 0.04 \times 10^{-5} \text{K}^{-1}$  from Fig. 5, respectively.

Using the Eq. 13 of Birch–Murnaghan-expansion VPT TEOS, pressures are predicted and listed in Table 1 as “VPT TEOS predicted P (GPa)”, and plotted in Fig. 6 as VPT TEOS. The predicted pressures are around  $0.1 \pm 0.1$  GPa and have a flat trend throughout the entire experimental temperature range, and match with the experimental data very well. The error propagation of variation of both VPT pressure predicted and PVT pressure predicted in this project are only from the volume variation, none of them from variation of bulk modulus, pressure derivative bulk

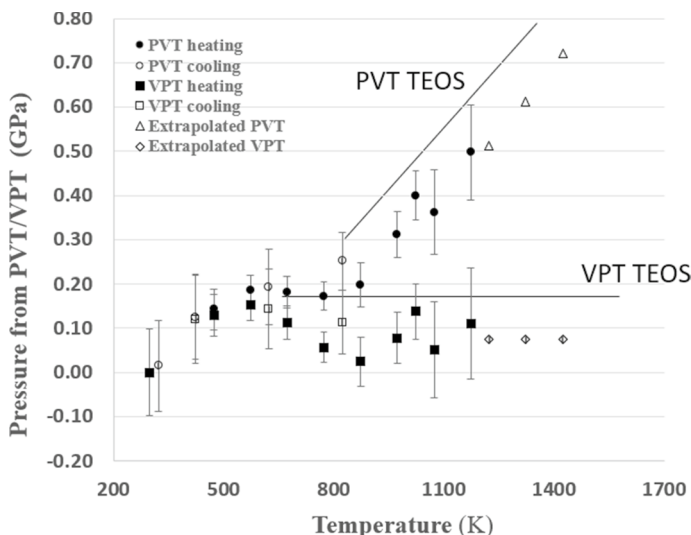


**Fig. 6** The pressure calculated from Birch–Murnaghan-expansion VPT TEOS and Birch–Murnaghan-Anderson PVT TEOS based on the experimental volume and temperature values, of solid MgO at ambient pressure in Table 1. The trend line of Birch–Murnaghan-Anderson PVT TEOS and Birch–Murnaghan-expansion VPT TEOS are displayed, respectively

modulus, etc. It looks like there is a bump around 550 K for the pressure prediction from both Birch–Murnaghan-expansion VPT TEOS and Birch–Murnaghan-Approximated Anderson PVT TEOS. The reason might be that the room temperature data point is the reference point, so there is least deviation at this point.

The VPT TEOS formulations Eqs. 8, 12, and Birch–Murnaghan-expansion Eq. 13 are supposed to be applicable to high pressure, but due to lack of pressure dependent thermal expansion coefficients at high P–T for most common pressure calibrants, validation of Birch–Murnaghan-expansion VPT TEOS for high pressure cannot be provided at the moment in this report.

### 5.3 Prediction from Birch–Murnaghan-Approximated Anderson PVT TEOS

The Anderson thermal pressure model is the original and widely used model for thermal pressure. As mentioned before, since both  $\alpha_p$  and  $K_T$  are pressure and temperature dependent, the integration of product of  $\alpha_p \cdot K_T$  not straightforward, and approximated to  $\alpha_0 \cdot K_0$ . Combined the most common 3<sup>rd</sup> order Birch–Murnaghan equation and approximated Anderson thermal pressure model, the thermal equation of state is expressed below, called Birch–Murnaghan-Approximated Anderson PVT TEOS,

$$P_{V,T} = \frac{3K_0}{2} \left[ \left( \left( \frac{V_0}{V} \right)^{\frac{2}{3}} \right) - \left( \frac{V_0}{V} \right)^{\frac{5}{3}} \right] \left\{ 1 + \frac{3}{4} (K'_0 - 4) \left[ \left( \left( \frac{V_0}{V} \right)^{\frac{2}{3}} \right) - 1 \right] \right\} + \alpha_0 \cdot K_0 (T - T_0). \tag{14}$$

Inputting the same  $K_0$ ,  $K'_0$ ,  $V_0$ ,  $\alpha_0$ , and experimental volume and temperature value of MgO in Table 1, the predicted pressures from Birch–Murnaghan-Approximated Anderson PVT TEOS are calculated from Eq. 14, listed as “PVT TEOS predicted P (GPa)” in Table 1 and plotted in Fig. 6 as PVT heating/cooling. According to the Fig. 6, the pressure prediction from Birch–Murnaghan-approximated Anderson PVT TEOS overestimates the pressure values, and the higher the temperature, the bigger the deviation. The approximated PVT TEOS exhibits a wrong upward trend from the real ambient pressure of zero (0) GPa. The main deviation might be from the approximation of  $\alpha_p \cdot K_T$  to  $\alpha_0 \cdot K_0$ .

Not only does the MgO data in this project validates the Birch–Murnaghan-expansion VPT TEOS model, but the data of gold (Au) from literature does as well. For details of Au data, please refer to the supplemental material. Both Au and MgO Birch–Murnaghan-expansion VPT TEOS have a flat trend that matches with experimental data of zero (0) GPa in the whole experimental range, while pressure prediction from the approximated traditional PVT TEOS shows a wrong trend.

In summary, from the experimental data of volume and temperature, Birch–Murnaghan-expansion VPT TEOS model predicted pressure matches the ambient pressure of zero (0) GPa very well. On the contrary, the pressure prediction from the approximated Anderson PVT TEOS exhibit a big deviation and a wrong trend. It would be more convincing to prove Birch–Murnaghan-expansion VPT TEOS at high pressure. But unlike the case of ambient pressure (zero (0) GPa) are well-known, there is a big discrepancy of the pressure scale at high pressure, so, the validation of VPT TEOS for high pressure cannot be provided at the moment.

## 6 Conclusion

In the PVT thermal equation of state, thermal pressure is the pressure change in an isochoric heating process. It is the pressure pushing the sample's volume back to the volume prior to heating. In this report, it is demonstrated that (1) One heating followed by a pressure adjusting could make isochoric heating, but any single high pressure heating in a DAC is not an isochoric heating, so the pressure change in a non-isochoric process is not exactly the thermal pressure. (2) The thermal pressure cannot be determined by the thermal pressure of its calibrant. Without direct experimental thermal pressure, temperature dependent  $K_T$  in the Anderson thermal pressure model and Grüneisen parameter in the Mie–Grüneisen thermal pressure model cannot be fitted easily and accurately. In this report, it is proposed to substitute the thermal pressure model with the thermal expansion model. Integrating any isothermal compression model at room temperature with the thermal expansion model at high pressure yield an alternative VPT TEOS model. The Birch–Murnaghan-expansion VPT TEOS were proved by MgO and Au at ambient pressure. Since there is limited high pressure  $\alpha_p$  for most calibrants at the moment, verifications of VPT TEOS at high P–T range is desirable in future research.

**Supplementary Information** The online version contains supplementary material available at <https://doi.org/10.1007/s10765-022-03089-8>.

**Acknowledgments** JY thanks the reviewing and comments from Raymond Jeanloz, Yingwei Fei, Bin Chen, Budhiram Godwal, et al. JY thanks the discussions with Quentin Williams, Andrew Doran, Fang Hong, Binbin Yue, and Mingqiang Hou, Qiaoshi Zeng, Qingyang Hu. We thank Richard Haase, Ph.D., from Edanz Group ([www.edanzediting.com/ac](http://www.edanzediting.com/ac)) for editing a draft of this manuscript.

**Author Contributions** JY wrote the manuscript, conducted the data acquisition, and data reduction. SY and JY revised the manuscript.

**Funding** JY was supported by COMPRES, the Consortium for Materials Properties Research in Earth Sciences under NSF Cooperative Agreement EAR 1606856. The Advanced Light Source is supported by the Director, Office of Science, Office of Basic Energy Sciences, of the U.S. Department of Energy under contract No. DE-AC02-05CH11231. SY acknowledges partial support from NSF EPSCoR CIMM project under award No. 1541079, CIMM LINK project, NSF EPSCoR LAMDA (No. OIA-1945231) SEED award No. LEQSF-EPS(2021)-LAMDASeed-Track1B-04, NSF award No. 2216805, DOE/NNSA award No. DE-NA0003979, and DoD support under contract No. W911NF1910005.

**Data Availability** All data can be provided upon request.

## Declarations

**Conflict of interest** The authors declare that they have no conflict of interest.

**Open Access** This article is licensed under a Creative Commons Attribution 4.0 International License, which permits use, sharing, adaptation, distribution and reproduction in any medium or format, as long as you give appropriate credit to the original author(s) and the source, provide a link to the Creative Commons licence, and indicate if changes were made. The images or other third party material in this article are included in the article's Creative Commons licence, unless indicated otherwise in a credit line to the material. If material is not included in the article's Creative Commons licence and your intended use is not permitted by statutory regulation or exceeds the permitted use, you will need to obtain permission directly from the copyright holder. To view a copy of this licence, visit <http://creativecommons.org/licenses/by/4.0/>.

## References

1. Y. Fei, J. Li, K. Hirose, W. Minarik, J.V. Orman, C. Sanloup, W.V. Westrenen, T. Komabayashi, K. Funakoshi, *Phys. Earth Planet. Inter.* **143–144**, 515 (2004)
2. Y. Wang, T. Uchida, J. Zhang, M.L. Rivers, S.R. Sutton, *Phys. Earth Planet. Inter.* **143**, 57 (2004)
3. K. Hirose, S. Karato, V.F. Cormier, J.P. Brodholt, D.A. Yuen, *Geophys. Res. Lett.* **33**, L12S01 (2006)
4. Y. Ye, V. Prakapenka, Y. Meng, S.H. Shim, *J. Geophys. Res.: Solid Earth* **122**, 3450 (2017)
5. G. Fiquet, J.P. Itie, P. Richet, D. Hausermann, M. Hanfland, D. Andrault, *Eur. J. Mineral.* **10**, 931 (1998)
6. D. Belmonte, *Minerals* **7**, 183 (2017)
7. E.D.J. Evans, *Phys. Lett. A* **91**, 457 (1982)
8. A.I. Burshtein, *Introduction to Thermodynamics and Kinetic Theory of Matter* (Wiley, Mörlenbach, 2008)
9. D.L. Heinz, *Geophys. Res. Lett.* **17**, 1161 (1990)
10. B. Kiefer, T.S. Duffy, *J. Appl. Phys.* **97**, 114902 (2005)
11. T.J.B. Holland, R.J. Powell, *J. Metamorph. Geol.* **29**, 333 (2011)
12. O.L. Anderson, D. Isaack, H. Oda, *Rev. Geophys.* **30**, 57 (1992)
13. O.L. Anderson, *Equations of State of Solids for Geophysics and Ceramic Science. Oxford Monographs on Geology and Geophysics No. 31* (Oxford University Press, New York, 1995)
14. R.E. Hanneman, H.C. Gatos, *J. Appl. Phys.* **36**, 1794 (1965)
15. B.B. Karki, R.M. Wentzcovitch, S. de Gironcoli, S. Baroni, *Phys. Rev. B* **61**, 8793 (2000)

16. R.J. Angel, F. Miozzi, M. Alvaro, *Minerals* **9**, 562 (2019)
17. O.L. Anderson, E. Schreiber, R.C. Liebermann, N. Soga, *Rev. Geophys.* **6**, 491 (1968)
18. Q. Williams, E. Knittle, R. Jeanloz, *J. Geophys. Res.: Solid Earth* **96**, 2171 (1991)
19. R. Fischer, A.J. Campbell, O.T. Lord, G.A. Shofner, P. Dera, V.B. Prakapenka, *Geophys. Res. Lett.* **38**, L24301 (2011)
20. W.A. Bassett, *High Press. Res.* **29**, 163 (2009)
21. I.M. Chou, J.G. Blank, A.F. Goncharov, *Science* **281**, 809 (1998)
22. W.F. Lewis, D. Benson, R.K. Crawford, W.B. Daniels, *J. Phys. Chem. Solids* **35**, 383 (1974)
23. T.G. Plymate, J.H. Stout, *Phys. Chem. Miner.* **21**, 413 (1994)
24. G. Shen, P. Lazor, S.K. Saxena, *Phys. Chem. Miner.* **20**, 91 (1993)
25. Z. Wang, Y. Liu, Y. Bi, W. Song, H. Xie, *High Press. Res.* **32**, 167 (2012)
26. W.R. Panero, R. Jeanloz, *J. Appl. Phys.* **91**, 2769 (2002)
27. J.C. Jamieson, J.N. Fritz, M.H. Manghnani, in *High Pressure Research in Geophysics*. ed. by S. Akimoto, M.H. Manghnani (D. Reidel Publishing Co., Boston, 1982), p.27
28. Y. Wang, D.J. Weidner, F. Guyot, *J. Geophys. Res.* **101**, 661 (1996)
29. Z.C. Jenei, *Rev. Sci. Instrum.* **84**, 095114 (2005)
30. J.S. Kreutz, *Phys. Rev. B* **72**, 214115 (2005)
31. V.L. Solozhenko, *J. Superhard Mater.* **39**, 71 (2017)
32. R.L. Cook, H.E. King Jr., C.A. Herbst, D.R. Herschbach, *J. Chem. Phys.* **100**, 5178 (1994)
33. V. Iota, C. Yoo, J. Klepeis, Z. Jenei, W. Evans, H. Cynn, *Nat. Mater.* **6**, 34 (2007)
34. Z.A. Dreger, C.J. Breshike, Y.M. Gupta, *Chem. Phys. Lett.* **679**, 212 (2017)
35. N. Dubrovinskaia, L. Dubrovinsky, Chapter 25. Internal and external electrical heating in diamond anvil cells, in *Advances in High-Pressure Technology for Geophysical Applications*. ed. by J. Chen, Y. Wang, T.S. Duffy, G. Shen, L.P. Dobrzhinskaya (Elsevier Science, Amsterdam, 2005), pp.487–501
36. Y.C. Zhao, F. Porsch, W.B. Holzapfel, *Phys. Rev. B* **52**, 134 (1995)
37. J. Zhang, Y. Zhao, R.S. Hixson, G.T. Gray, *Phys. Rev. B* **78**, 054119 (2008)
38. F. Datchi, A. Dewaele, Y.L. Godec, P. Loubeyre, *Phys. Rev. B* **75**, 214104 (2007)
39. J. Yan, S. Yang, Pressure dependent thermal expansion coefficient by a diamond anvil cell. *Int. J. Thermophys.* (2022). <https://doi.org/10.1007/s10765-021-02945-3>(2021)
40. Y. Fei, Thermal expansion, in *Mineral physics and crystallography. A handbook of physical constants*. ed. by T.J. Ahrens (American Geophysical Union, Washington, 1995)
41. D.T.A. Duffy, Pressure-volume-temperature equations of state, Argonne National Lab. (ANL), Argonne, IL (United States). Advanced Photon Source (APS) (2003)
42. R.J. Angel, Equations of state, in *High pressure and high temperature crystal chemistry*. ed. by R.M. Hazen, R.T. Downs (De Gruyter, Berlin, 2000), p.35
43. F.D. Murnaghan, *Am. J. Math.* **59**, 235 (1937)
44. J. Freund, R. Ingalls, *J. Phys. Chem. Solids* **50**, 263 (1989)
45. J.P. Poirier, A. Tarantola, *Phys. Earth Planet. Inter.* **109**, 1 (1998)
46. P.J.J.R. Vinet, J. Ferrante, J.R. Smith, J.H. Rose, *J. Phys. C: Solid State Phys.* **19**, L467 (1986)
47. F. Birch, *Phys. Rev.* **71**, 809 (1947)
48. R.J. Angel, M. Alvaro, F. Nestola, *Phys. Chem. Miner.* **45**, 95 (2018)
49. H. Kroll, A. Kirfel, R. Heinemann, B. Narbier, *Eur. J. Mineral.* **24**, 935 (2012)
50. M. Kunz, J. Yan, E. Cornell, E.E. Domning, C.E. Yen, A. Doran, C.M. Beavers, A. Treger, Q. Williams, A.A. MacDowell, *Rev. Sci. Instrum.* **89**, 083903 (2018)
51. A. Doran, L. Schlicker, C.M. Beavers, S. Bhat, M.F. Bekheet, A. Gurlo, *Rev. Sci. Instrum.* **88**, 013903 (2017)
52. B. Bochu, J. Laugier, Laboratoire des Matériaux et du Génie Physique, Ecole Nationale Supérieure de Physique de Grenoble (INPG), Grenoble, France (1999)
53. G. Fiquet, P. Richet, G. Montagnac, High-temperature thermal expansion of lime, periclase, corundum and spinel. *Phys. Chem. Miner.* **27**(2), 103–111 (1999)
54. J. Zhang, *Phys. Chem. Miner.* **27**, 145 (2000)